

# Merging Bond Graph and Signed Directed Graph to improve FDI procedure

N. Chatti, B. Ould-Bouamama, A-L. Gehin, and R. Merzouki\*

## Abstract

*The Fuel Cell (FC) is an ideal electrical power source. However, FC stacks and even more FC systems are vulnerable to faults (such as water flooding and membrane drying) that can cause the disruption or the permanent damage. To guarantee the safe operation of the FC systems, it is necessary to use systematic techniques to detect and isolate faults for the purpose of diagnosis. The problematic for the model-based Fault Detection and Isolation (FDI) of fuel cell is that the model is complex because of coupling multiple physical domains (electrochemical, electrical, thermofluidic...). This is why, we propose in this paper, the exploitation of the behavioral and structural properties of the Bond Graph (BG) as a multi-domain power exchange and unified graphical modeling language for qualitative analysis of monitoring ability (using Signed Directed Graph properties). This is obtained after generation of the fault indicators from one part, and by dealing with an automatically built Signed Directed Graph (SDG) of the system, from another part. By combining qualitative method (based on Signed Graph) and quantitative method (fault indicator generation) using only one representation, an innovative approach to perform (single and multiple faults) diagnosis is proposed. The proposed contribution is illustrated by an application to a Proton Exchange Membrane Fuel Cell (PEMFC).*

## 1. INTRODUCTION

Much attention has been paid during this last decade to fuel cells because they offer significant advantages such as a high efficiency and an environmentally friendly technology for energy conversion [1].

\*This work was supported by the European Project InTraDE (Intelligent Transportation for Dynamic Environment), Interreg IVB, 091C North West Europe Zone.

†The authors are with Polytech' Lille, LAGIS, CNRS-UMR 8219, 59655 Villeneuve d'Ascq, France (e-mail: nizar.chatti@polytech-lille.fr; belkacem.oudbouamama@polytech-lille.fr; anne-lise.gehin@polytech-lille.fr; rochdi.merzouki@polytech-lille.fr)

Among many varieties of fuel cells, the PEMFC has shown to be the most promise for various industries including the transportation, residential and also portable applications. It is the fuel cell that is the most likely to be widely used in the near future. This issue leads to the question: what is lacking in order to enable a widespread use of fuel cells?

Indeed, PEM fuel cells are not without challenges and several issues need to be resolved before fuel cells can be commercially viable. To improve fuel cell lifetime and develop adequate mitigation strategies, different working parameters should be measured and monitored to minimize the risk of damaging the fuel cell. However, PEM fuel cell fault diagnosis requires the knowledge of a number of fundamental physical phenomena and the description of their dynamic behaviors. This is why, their modeling has become more and more important over the years in order to simulate the behaviour of the fuel cell integrated in a power system. The literature contains several research publications on modeling, simulation and experimental validation of a PEM fuel cell system [2]. For an overview of PEM fuel cells diagnosis approaches, Wu et al. [3] review various diagnostic tools in PEM fuel cell and electrochemical techniques. They also outline the principle, experimental implementation, and data processing of each technique.

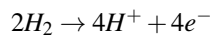
Roughly speaking, fuel cell systems are still badly known, particularly when talking about fault diagnosis. This is why, a diagnosis strategy to detect and classify failures or faulty operation modes so as to prevent or limit degradation, is required. In fact, we can distinguish between reversible and irreversible faults. Some problems associated with the PEM fuel cell include irreversible degradation such as membrane degradation due to mechanical phenomena, corrosion or chemical contamination. Other degradations are reversible such as the membrane drying, the cathode flooding and the anode catalyst poisoning by carbon monoxide [4][5]. Basically, in this paper we focus on the degradations linked with water management (flooding and mem-

brane drying) which are of particular interest because an unsuitable water balance (either too wet or too dry) has a long term effect on cell degradation rates and it is essential to not only detect such fault but to isolate it in order to be able to overcome the exposure to excess water or dryness which can lead to irreversible degradations of the cell. Furthermore, from the Failure Modes and Effects Analysis (FMEA), used off line for analysis of potential failure modes within a FC system, it was shown [6] that the state of hydration of the membrane electrode assembly (water flooding and drying) is one of the major challenges in PEMFCs diagnosis. There are many different approaches for fault diagnosis. These approaches are based on experimental data [7], signal processing [8] and analytical models [9].

In this paper, we propose an heterogeneous diagnosis approach for fuel cell, which combines between a qualitative signed graph model-based method and a quantitative bond graph model-based method. The innovative interest of the presented paper is the use of only one representation for not only structural modeling but also for diagnosis of single and multiple faults which may affect the fuel cell. The paper is organized as follows. The fuel cell principle is described in section 2 and the corresponding Word Bond Graph is given in section 3. The proposed diagnosis approach is presented in section 4 and applied on the fuel cell is section 5. Section 6 concludes the paper.

## 2. Fuel Cell description

A fuel cell is a device that produces electricity from a chemical reaction. This reaction generates electrical current (which can be directed outside the cell to power an electrical motor for example) and requires a fuel (namely hydrogen) and oxygen. As shown in Fig.1, the fuel cell consists of a membrane sandwiched between two electrodes namely the anode and the cathode. The hydrogen passes over the anode and with help of a catalyst, is separated into hydrogen protons and electrons. The chemical reaction in the anode is:



Then, the membrane plays a key role because it permits the protons  $H^+$  to pass between the anode and the cathode while filtering the electrons. This is why, the protons flow to the cathode through the membrane while the electrons flow through an external circuit, thus creating electricity. On the other hand, oxygen enters the fuel cell at the cathode and it combines with electrons (returning from the external circuit) and hydrogen protons (that flow through the membrane

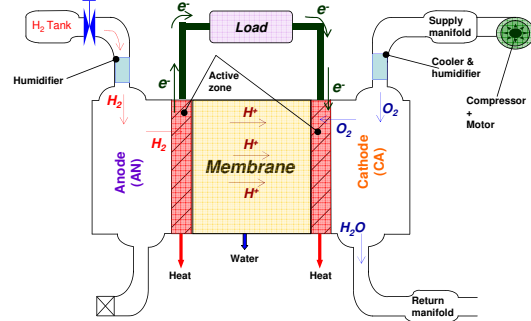
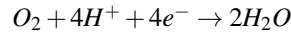
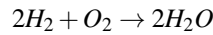


Figure 1. Fuel cell principle

from the anode), and produce water and heat. Thus, the chemical reaction in the cathode is:



The overall reaction of the fuel cell is therefore:



The PEM fuel cell is the heart of the fuel cell. However, as shown in Fig.1, other subsystems are interacting within the fuel cell stack system and are as follows:

- The  $H_2$  valve is used to control the flow rate of hydrogen.
- From the anode side, the Humidifier is used to humidify the hydrogen flow.
- From the cathode side, the Humidifier add vapor into the air flow in order to prevent drying of the membrane.
- The air Cooler is needed to reduce the air temperature before it enters the stack.
- The air supply system has a compressor motor command as the only control actuator.
- The return manifold represents the pipeline at the fuel cell stack water exhaust.

## 3. Word Bond Graph

In this section, we present the fuel cell system's Word Bond Graph which represents the technological level of the model where global system is decomposed into different subsystems (see Fig.2). This representation is deduced from the analysis of the fuel cell operating as described in the previous section. Comparing to classical block diagram, the input and output of each subsystem define power variables represented by

a conjugated pair of effort-flow labelled by a half arrow. Indeed, the Word Bond Graph provides a top-level overview of the fuel cell system and is useful for initial conception of the behavioral system model. Power variables used for the studied fuel cell system are: (Torque, angular velocity) =  $(\tau, \omega)$ , (Pressure, Mass Flow) =  $(P, \dot{m})$ , (Temperature, Enthalpy Flow) =  $(T, \dot{H})$ , (chemical potential, molar flow) =  $(\mu, \dot{n})$  and (Voltage, Current) =  $(U, i)$ . These variables are associated respectively with mechanical, hydraulic, thermal, chemical and electrical domains. Because of the complexity of the overall system and for the sake of clarity, we will focus within this paper only on the heart of the fuel cell system model.

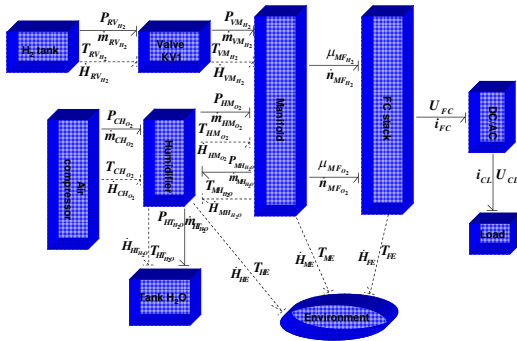


Figure 2. Word Bond Graph of the PEM fuel cell system

#### 4. Proposed diagnosis approach

The diagnosis approach, we propose, rests on two parts. In a first time, models and tools required for on line diagnosis are designed. In a second time, models and tools previously built are on-line exploited in order to detect and isolate faults.

##### 4.1. Design of the diagnosis module

The design of the diagnosis module rests on four steps which are illustrated in Fig.3 and summarized as follows. In a first step, the BG model is built based on the physical system architecture and the power exchanges between the different components. Background material on bond graphs modeling can be found in [10]. An example of BG in given by Fig.6. It will be detailed later. We just remind here basic notions.

A BG combines vertices and power bonds. Power bonds are oriented to represent the direction of the power transfer between vertices and are associated with two variables: the effort (above the bond) and the flow (below the bond). Moreover to be numerical pro-

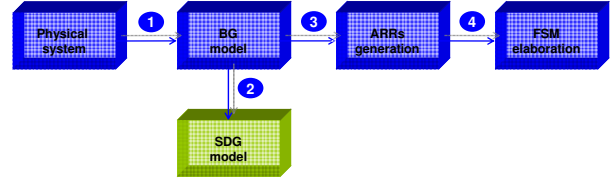


Figure 3. Design step

BG model	Associated SDG	BG model	Associated SDG
$S_e : v(t) \xrightarrow{1}$ $S_f : v(t) \xrightarrow{1}$	$(e_1 \rightarrow f_1)$ $(e_1 \rightarrow f_1)$	$D_{f_1} \xrightarrow{1}$ $D_{e_1} \xrightarrow{1}$	$(f_1 \rightarrow e_1)$ $(e_1 \rightarrow f_1)$
$\xrightarrow{1} R : R_i$	$(f_1 \rightarrow e_1)$ $(e_1 \rightarrow f_1)$	$\xrightarrow{1} R : R_i$	$(f_1 \rightarrow e_1)$ $(e_1 \rightarrow f_1)$
$\xrightarrow{1} I : L_i$	$(f_1 \rightarrow e_1)$ $(e_1 \rightarrow f_1)$	$\xrightarrow{1} I : L_i$	$(f_1 \rightarrow e_1)$ $(e_1 \rightarrow f_1)$
$\xrightarrow{1} C : C_i$	$(f_1 \rightarrow e_1)$ $(e_1 \rightarrow f_1)$	$\xrightarrow{1} C : C_i$	$(f_1 \rightarrow e_1)$ $(e_1 \rightarrow f_1)$
$\xrightarrow{1} TF : n \xrightarrow{2}$	$(f_1 \rightarrow e_1)$ $(e_1 \rightarrow f_2)$ $(f_2 \rightarrow e_1)$	$\xrightarrow{1} TF : n \xrightarrow{2}$	$(f_1 \rightarrow e_1)$ $(e_1 \rightarrow f_2)$ $(f_2 \rightarrow e_1)$
$\xrightarrow{1} GV : r \xrightarrow{2}$	$(f_1 \rightarrow e_1)$ $(e_1 \rightarrow f_2)$ $(f_2 \rightarrow e_1)$	$\xrightarrow{1} GV : r \xrightarrow{2}$	$(f_1 \rightarrow e_1)$ $(e_1 \rightarrow f_2)$ $(f_2 \rightarrow e_1)$
$\xrightarrow{1} 0 \xrightarrow{2}$	$(f_1 \rightarrow f_2)$ $(f_1 \rightarrow f_2)$	$\xrightarrow{1} 1 \xrightarrow{2}$	$(e_1 \rightarrow e_2)$ $(e_1 \rightarrow e_2)$

Figure 4. BG to SDG transformations.

cessed, the BG model is exploited to directly generated a Signed Directed Graph (SGD) using the correspondences given by the table represented on Fig.4. A SDG is a digraph used to represent the causal relationships between process variables. It was introduced by Iri et al. [11] for fault diagnosis in the chemical process industries. Process variables are represented by nodes and the cause/effect relationship between two variables is represented by a directed arc between the corresponding nodes. The source node of an arc is the cause and the destination node is the effect. Each node is assigned with a sign from the set  $\{0, +, -\}$  respectively when the deviation of a measured value of the variable from its previous steady value is between the thresholds boundaries, bigger than the maximal threshold or smaller than the minimal one. Positive or negative influence between nodes is distinguished by the sign  $'+'$  or  $'-'$  of the arc, shown as a solid or dotted arc respectively. This automatically generation of the SDG from the BG is given by Fig.4. This transformation overcomes the difficulty of its elaboration and of its posteriori validation. An example of SDG graph is given by Fig. 7. It will be detailed later.

## 4.2. On-line exploitation of the diagnosis module

The on-line diagnosis procedure is illustrated in Fig.5 and is summarized as follows. In a first time, measured outputs and control inputs which represent the known variables are used to calculate the value of the coherence vector from the ARR from one part, and to determine the sign of the measured nodes of the SDG from another part. In the normal operating mode, the value of the coherence vector is equal to  $(0, 0, \dots, 0)$  and all nodes of the SDG take the value of zero. When a fault appears, the value of the coherence vector is different from  $(0, 0, \dots, 0)$  and is compared to the fault signature regrouped in the Fault Signature Matrix (FSM). This leads to a list of potential faults and allows the extraction of a subgraph from the entire SDG graph. This last, is then analyzed to extract potential abnormal situations. Indeed, on the SGD graph, the fault node first changes sign, then it will be propagated along directed arcs throughout the whole graph. SDG diagnosis aims to identify the fault origin node (component responsible of the fault) from the valid nodes and the consistent paths of the graph. A valid node is a node which is affected by a value different from '0'. It represents the fault information. A consistent path is a path which can propagate the fault information. It consists of consistent arcs. An arc is said consistent if its value is equal to the product of the values of the two linked nodes. To extract the consistent paths a bidirectional inference algorithm is used. Starting from the nodes which are detected as faulty ones (the associated measured values are not in the thresholds boundaries), adjacent arcs are followed whatever their direction to determine the sign of their destination nodes. The same procedure is applied until all nodes which correspond to a measured output or an input control are reached with respect of their corresponding signs. Two types of paths are extracted, paths which include hardware components and paths which do not include hardware components. The consistency analysis between these two types of paths allows to reject or to isolate candidate potential faults. If consistency there is, some faults may be isolated. In the opposite case, a partial result is given (see Fig.5).

## 5. Diagnosis of the PEM fuel cell

The BGs have been successfully used for analysis and synthesis of different kinds of systems involving multiphysical phenomena. Hence an easier understanding of the overall system. Fig. 6 presents the proposed BG model of the PEM fuel cell system. The transformers  $TF_{an}$ ,  $TF_{ca}$ ,  $TF_{ca2}$  represent chemical transforma-

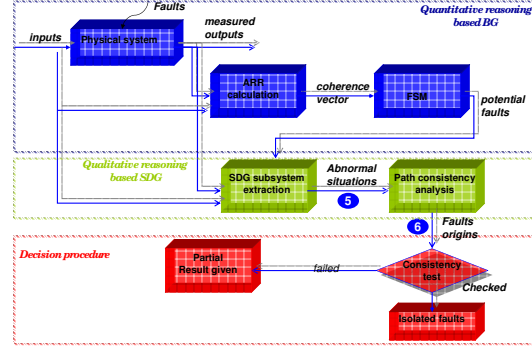


Figure 5. On line exploitation

tions related respectively to the hydrogen flow through the anode, the oxygen flow through the cathode and the water flow through the cathode. On the other hand,  $TF_e$  represents the transformation of the variations of the enthalpies, or the Gibbs free energy, into electrical energy and wherein  $n$  is the number of free electrons and  $F$  is the Faraday constant. The 1-junctions represent conservation law energy. The multiport  $R : R_c$  modulated by mass flow is used to model the coupling of fluidic and thermal energies.  $D_e$  and  $D_f$  (sensors) represent respectively the effort detector and flow detector.  $S_e$  and  $S_f$  represent respectively the effort source and flow source.  $R_v$  represents the inlet  $H_2$  valve which is modeled hence by hydraulic resistance.  $R_t$  and  $R_c$  represent the friction of the diffusion through the surface of the backing layer respectively for the  $H_2$  and  $O_2$ . The thermal losses are modeled by an active resistance element-RS such as activation losses, diffusion losses, concentration losses, ohmic losses ...

Let focus on Fig.6 in order to deduce the ARRs: From the *Junction*( $1_1$ ), the following equations can be written:

$$e_1 - e_2 - e_3 = 0 \quad (1)$$

$$e_1 = P_{H_2} \quad (2)$$

$$e_2 = f(f_2, x) \quad (3)$$

$$f_2 = f_3 = \dot{m} \quad (4)$$

$$e_3 = e_4 = P_v \quad (5)$$

From equations (1), (2), (3), (4) and (5), we can deduce the first ARR as follows:

$$P_{H_2} - f(f_2, x) - P_v = 0 \quad (6)$$

Similarly, from the junction( $1_3$ ), we can write:

$$e_9 - e_{10} - e_{11} - e_{12} - e_{13} - e_{14} - e_{15} = 0 \quad (7)$$

$$e_{10} = f_{10} \times RS_{an}; e_{11} = f_{11} \times RS_{act}; e_{12} = f_{12} \times RS_{mem} \quad (8)$$

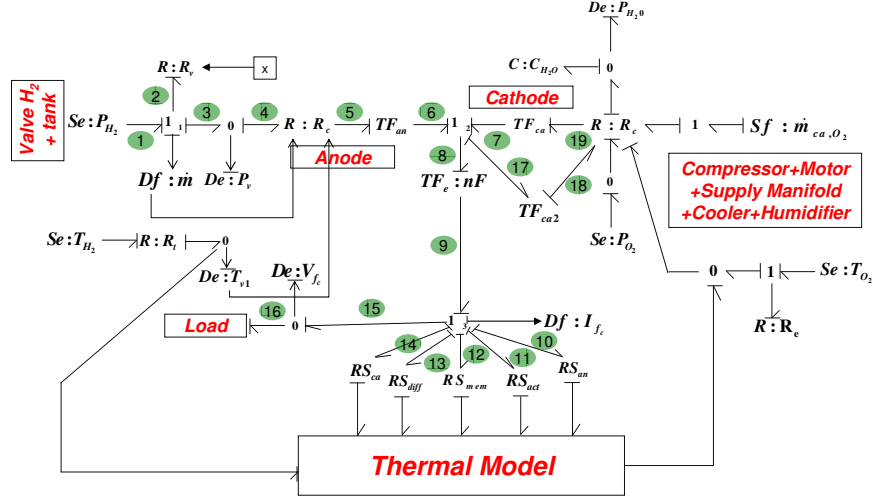


Figure 6. Bond Graph model of the PEM fuel cell system

$$e_{13} = f_{13} \times RS_{diff}; e_{14} = f_{14} \times RS_{ca}; e_{15} = V_{fc} \quad (9)$$

$$f_{10} = f_{11} = f_{12} = f_{13} = f_{14} = I_{fc} \quad (10)$$

$$e_8 = nF \times e_9 \quad (11)$$

$$e_{19} = f(P_{O_2}, T_{O_2}); P_{O_2} = f(\dot{m}_{O_2}, P_{out}); e_5 = f(T_{v1}, e_4) \quad (12)$$

$$e_5 = e_6; e_{18} = f(P_{H_2O}, T_{H_2O}) \quad (13)$$

From equations (7) to (13), the second ARR is then deduced:

$$f(T_{v1}, P_v) + f[f(\dot{m}_{O_2}, P_{out}), T_{O_2}] - nF[I_{fc} \times (RS_{act} + RS_{diff} + RS_{ca} + RS_{an} + RS_{mem}) + V_{fc}] - f(P_{H_2O}, T_{H_2O}) = 0 \quad (14)$$

From junction(12) and by following the same procedure, the third ARR can be obtained as follows:

$$\frac{1}{nF} [f(T_{v1}, P_v) + f(P_{O_2}, T_{O_2}) - f(P_{H_2O}, T_{H_2O})] - I_{fc} \times (RS_{act} + RS_{diff} + RS_{ca} + RS_{an} + RS_{mem}) - V_{fc} = 0 \quad (15)$$

The fault signature matrix (FSM) is derived directly from these three ARRs namely (6), (14) and (15). It is given in Table 1. The vector (R1, R2, R3) is the

signature of the fault. The only isolated faults are those having the same signature, i.e. different from the signatures of all other element (such as the signature  $V=(1, 1, 1)$  corresponding to the  $H_2$  pressure sensor). However, due to the non presence of enough unique signatures, faults affecting the other elements can not be isolated. This is why, as previously explained, the SDG is introduced. Let now focus, for instance, on the faults corresponding to water management (flooding and drying). The signature  $V = (0, 0, 1)$  corresponding to those faults is not unique. However, the deduced signed graph is used to improve the fault isolability performance. Indeed, when the signature  $V = (0, 0, 1)$  is observed, the flooding of the cathode induces an increase of the value related to the cathode pressure  $P_{H_2O}$  which becomes  $P_{H_2O}(+)$  because it exceeds a certain threshold. On the other hand, the value of the current  $I_{fc}$  decreases and becomes  $I_{fc}(-)$ . As shown in Fig.7 which corresponds to the deduced Signed Graph, the only consistent path explaining those observations is as follows:

$$P_{H_2O}(+) \rightarrow e_{17}(+) \rightarrow e_8(-) \rightarrow e_9(-) \rightarrow V_{fc}(-) \rightarrow e_{12}(+) \rightarrow I_{fc}(-) \quad (16)$$

This consistent path shows (from observations) that the resistance  $R_{mem}$  is not involved in the fault origin. However, the resistance is sensitive to the drying of the membrane. Hence, we can deduce that the fault concerns flooding of the cathode despite the fact that we do not have any sensor inside the membrane to measure the resistance of the membrane. Let consider now the scenario wherein the signature  $V = (0, 0, 1)$  is observed as well. The value of the current  $I_{fc}$  exceeds a cer-

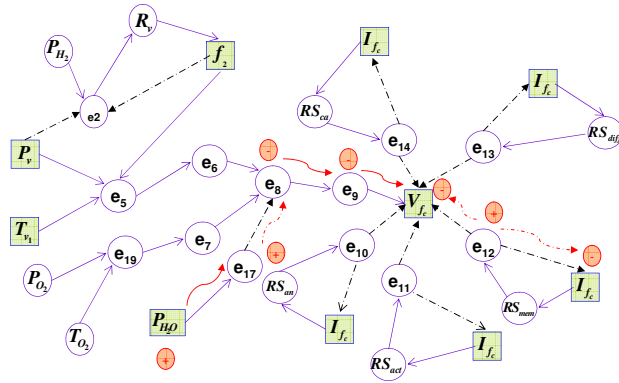


Figure 7. Deduced Signed Directed Graph

Fault	$R_1$	$R_2$	$R_3$	$D$	$I$
Drying of the membrane	0	0	1	1	0
Flooding of the cathode	0	0	1	1	0
$H_2$ valve regulator	1	0	0	1	0
$H_2$ mass flow sensor	1	0	0	1	0
$H_2$ pressure sensor	1	1	1	1	1
$H_2$ temperature sensor	0	1	1	1	0
Fuel cell current sensor	0	1	1	1	0
Fuel cell voltage sensor	0	1	1	1	0
Cathode water temperature sensor	0	1	1	1	0
Cathode water pressure sensor	0	1	1	1	0

Table 1. PEM Fuel cell Fault signature matrix

tain threshold and hence becomes  $I_{fc}(+)$ . The value of the pressure in the cathode  $P_{H_2O}$  increases as well and exceeds a certain threshold. From the deduced Signed Graph (Fig.7), the only consistent path explaining these variations is as follows:

$$\begin{aligned}
 P_{H_2O}(+) &\longrightarrow e_{17}(+) \longrightarrow e_8(-) \longrightarrow e_9(-) \longrightarrow \\
 V_{fc}(-) &\longrightarrow e_{12}(+) \longrightarrow RS_{mem}(+) \longrightarrow I_{fc}(+) \quad (17)
 \end{aligned}$$

Unlike the first case, we notice that the resistance of the membrane is sensitive to the fault. This is why, we can deduce from this qualitative propagation of the fault, that the fault is the drying of the membrane and hence we isolate the fault ( which is not possible when we rely only on the FSM).

## 6. CONCLUSION

A new approach has been presented for fault diagnosis of the PEM fuel cell. This approach is based on SDG and BG and allows to integrate two different types of information namely quantitative knowledge acquired from the behavioral, causal and structural features of the BG and qualitative knowledge based on SDG. By associating these two features, all built on the same model: the BG, we contribute to the development of a global

FDI procedure which allows to detect and isolate faults within the PEM fuel cell. Indeed, the scenarii taken in the example illustrate the complementary of the different tools. The consistent path analysis performed on the SDG allows to isolate faults which are not isolable by the FSM analysis and the FSM analysis is required to extract the part of the SDG wherein the path consistency analysis has to be performed to give relevant results.

## References

- [1] A. Veziroglu and R. Macario, "Fuel cell vehicles: State of the art with economic and environmental concerns," *International Journal of Hydrogen Energy*, vol. 36, pp. 25 – 43, 2011.
- [2] K. Haraldsson and K. Wipke, "Evaluating pem fuel cell system models," *Journal of Power Sources*, vol. 126, pp. 88 – 97, 2004.
- [3] J. Wu, X. Zi Yuan, H. Wang, M. Blanco, J. Martin, and J. Zhang, "Diagnostic tools in pem fuel cell research: Part i electrochemical techniques," *International Journal of Hydrogen Energy*, vol. 33, pp. 1735 – 1746, 2008.
- [4] T. Kadyk, J., R. Hanke-Rauschenbach, Andrea-Novel, and K. Sundmacher, "Non linear frequency response analysis of pem fuel cells for diagnosis of dehydration, flooding and co-poisoning," *Journal of Electroanalytical Chemistry*, vol. 630, pp. 19 – 27, 2009.
- [5] M.-A. Rubio, A. Urquia, and S. Dormido, "Diagnosis of performance degradation phenomena in pem fuel cells," *International Journal of Hydrogen Energy*, vol. 35, pp. 2586 – 2590, 2010.
- [6] V. Anghel, "Prediction failure for pem fuel cells," *International Journal of Advances in Engineering & Technology*, vol. 4, pp. 1 – 14, 2012.
- [7] J. Wishart, Z. Dong, and M. Secanell, "Optimization of a pem fuel cell system based on empirical data and a generalized electrochemical semi-empirical model," *Journal of Power Sources*, vol. 161, pp. 1041 – 1055, 2006.
- [8] Z. Zhang, L. Jia, H. He, X. Wang, and L. Yang, "Modeling dynamic behaviors of a single cell proton exchange membrane fuel cell under different operating conditions," *Journal of the Taiwan Institute of Chemical Engineers*, vol. 41, pp. 689 – 698, 2010.
- [9] J. Chen and B. Zhou, "Diagnosis of pem fuel cell stack dynamic behaviors," *Journal of Power Sources*, vol. 177, pp. 83 – 95, 2008.
- [10] B. Ould-Bouamama, R. El Harabi, M.-N. Abdelkrim, and M.-K. Ben Gayed, "Bond graphs for the diagnosis of chemical processes," *Computers & Chemical Engineering*, vol. 36, pp. 301–324, 2012.
- [11] M. Iri, K. Aoki, E. O'shima, and H. Matsuyama, "An algorithm for diagnosis of system failures in the chemical process," *Computers & Chemical Engineering*, vol. 3, pp. 489–493, 1979.